SUBMITTED TO AJ 12/22/2003; REVISED VERSION SUBMITTED 02/24/2004; ACCEPTED 02/25/2004 FOR THE JUNE 2004 ISSUE
Preprint typeset using LaTeX style emulateapj v. 11/12/01

A LYMAN-α-ONLY AGN FROM THE SLOAN DIGITAL SKY SURVEY

PATRICK B. HALL,[1,2,3,4,5] ERIK A. HOVERSTEN,[6] CHRISTY A. TREMONTI,[7] DANIEL E. VANDEN BERK,[8] DONALD P. SCHNEIDER,[9] MICHAEL A. STRAUSS,[1] GILLIAN R. KNAPP,[1] DONALD G. YORK,[10] DAMIEN HUTSEMÉKERS,[5,11] P. R. NEWMAN,[12] J. BRINKMANN,[12] BRENDA FRYE,[1] MASATAKA FUKUGITA,[13] KARL GLAZEBROOK,[6] MICHAEL HARVANEK,[12] TIMOTHY M. HECKMAN,[6] ŽELJKO IVEZIĆ,[1] S. KLEINMAN,[12] JUREK KRZESINSKI,[12,14] DANIEL C. LONG,[12] ERIC NEILSEN,[15] MARTIN NIEDERSTE-OSTHOLT,[1] ATSUKO NITTA,[12] DAVID J. SCHLEGEL,[1] S. SNEDDEN[12]

ABSTRACT

The Sloan Digital Sky Survey has discovered a $z = 2.4917$ radio-loud active galactic nucleus (AGN) with a luminous, variable, low-polarization UV continuum, H I two-photon emission, and a moderately broad Lyα line (FWHM$\simeq$1430 km s^{-1}) but without obvious metal-line emission. SDSS J113658.36+024220.1 does have associated metal-line absorption in three distinct, narrow systems spanning a velocity range of 2710 km s^{-1}. Despite certain spectral similarities, SDSS J1136+0242 is not a Lyman-break galaxy. Instead, the Lyα and two-photon emission can be attributed to an extended, low-metallicity narrow-line region. The unpolarized continuum argues that we see SDSS J1136+0242 very close to the axis of any ionization cone present. We can conceive of two plausible explanations for why we see a strong UV continuum but no broad-line emission in this 'face-on radio galaxy' model for SDSS J1136+0242: the continuum could be relativistically beamed synchrotron emission which swamps the broad-line emission; or, more likely, SDSS J1136+0242 could be similar to PG 1407+265, a quasar in which for some unknown reason the high-ionization emission lines are very broad, very weak, and highly blueshifted.

Subject headings: quasars: general — quasars: emission lines — quasars: individual (SDSS J113658.36+024220.1, PG 1407+265)

1. INTRODUCTION

One of the goals of the Sloan Digital Sky Survey (SDSS; York et al. 2000) is to obtain spectra for $\sim 10^5$ quasars, in addition to the $\sim 10^6$ galaxies which comprise the bulk of the spectroscopic targets (Strauss et al. 2002; Blanton et al. 2003). From astrometrically calibrated drift-scanned imaging data (Gunn et al. 1998; Pier et al. 2003) on the SDSS *ugriz* AB asinh magnitude system (Fukugita et al. 1996; Lupton, Gunn, & Szalay 1999; Hogg et al. 2001; Stoughton et al. 2002; Smith et al. 2002), quasar candidates are selected primarily using color criteria designed to target objects whose broad-band colors differ from those of normal stars and galaxies (Richards et al. 2002a). Some of these quasars are bound to possess unusual properties.

Here we describe one such unusual quasar, SDSS J113658.36+024220.1 (hereafter SDSS J1136+0242), which exhibits strong Lyα emission but no detected metal-line emission. We discuss its unusual properties (§2), consider possible explanations for them (§3), and conclude with suggestions for further investigation (§4). Where needed, we assume H_0=70 km s^{-1} Mpc^{-1}, Ω_M=0.7 and Ω_Λ=0.3.

2. OBSERVATIONS AND PROPERTIES OF SDSS J1136+0242

2.1. *Photometry and Variability*

A catalog of observations and general properties of SDSS J1136+0242 is given in Table 1. Besides the SDSS imaging and spectroscopy, near-IR photometry was obtained on UT 2003 January 31 using the Infrared Side Port Imager (ISPI; Probst et al. 2003) on the CTIO 4-meter telescope, with total exposure times of 800 seconds in J and 300 seconds in K_s.

This object was imaged twice by the SDSS, and was unresolved in both epochs. A χ^2 analysis confirms variability

[1] Princeton University Observatory, Princeton, NJ 08544-1001

[2] Departamento de Astronomía y Astrofísica, Facultad de Física, Pontificia Universidad Católica de Chile, Casilla 306, Santiago 22, Chile; E-mail: phall@astro.puc.cl

[3] Guest Observer at the Cerro Tololo Inter-American Observatory, a division of the National Optical Astronomy Observatories, which is operated by AURA, Inc. under cooperative agreement with the National Science Foundation.

[4] Guest Observer at the Canada-France-Hawaii Telescope, a joint facility of the National Research Council of Canada, the Centre National de la Recherche Scientifique of France and the University of Hawaii.

[5] Guest Observer at the La Silla Observatory ESO 3.6m Telescope, for program 071.B-0460.

[6] Department of Physics and Astronomy, The Johns Hopkins University, 3400 North Charles Street, Baltimore, MD 21218-2686

[7] Steward Observatory, The University of Arizona, 933 North Cherry Avenue, Tucson AZ 85721

[8] Department of Physics and Astronomy, University of Pittsburgh, 3941 O'Hara Street, Pittsburgh, PA 15260

[9] Department of Astronomy and Astrophysics, The Pennsylvania State University, University Park, PA 16802

[10] Department of Astronomy and Astrophysics and Enrico Fermi Institute, The University of Chicago, 5640 S. Ellis Ave., Chicago, IL 60637

[11] Research Associate FNRS, University of Liège, Allée du 6 août 17, Bat. 5c, 4000 Liège, Belgium

[12] Apache Point Observatory, P.O. Box 59, Sunspot, NM 88349-0059

[13] University of Tokyo, Institute for Cosmic Ray Research, Kashiwa, 2778582, Japan

[14] Mt. Suhora Observatory, Cracow Pedagogical University, ul. Podchorazych 2, 30-084 Cracow, Poland

[15] Fermi National Accelerator Laboratory, P.O. Box 500, Batavia, IL 60510

between the two epochs of SDSS *ugriz* imaging data (with Δt=67 rest-frame days) at the 99.8% confidence level. Similarly, *gri* magnitudes synthesized from the spectroscopy differ at the 85% confidence level from the earlier SDSS imaging magnitudes (Δt=42 rest-frame days), but not from the later ones (Δt=25 rest-frame days). All imaging magnitudes come from data reduced with the same version of the SDSS photometric pipeline, and the spectroscopic comparison is empirically calibrated using observations of non-variable stars (Vanden Berk et al. 2004).

2.2. *Polarimetry*

Photopolarimetry of SDSS J1136+0242 was obtained on UT 2003 April 5 using the EFOSC instrument on the ESO 3.6m telescope at La Silla Observatory. SDSS J1136+0242 is unpolarized, with observed *i*-band (rest-frame $\sim$2300 Å) $P = 0.7 \pm 0.4\%$ at θ=155$\pm$19° E of N. The observed lack of polarization means that the observed continuum does not come from an elongated region surrounding the central source.

2.3. *Radio Emission*

SDSS J1136+0242 is a 1.44 mJy radio source in the FIRST survey (Becker, White, & Helfand 1995). Despite being near the FIRST flux limit, it appears marginally resolved in one dimension, with a deconvolved major axis extent of 6.″84 at position angle 74.4$\pm$3.9° E of N. The FIRST peak flux density is only 1.01 mJy, which is also suggestive of an extended source, though not conclusively so (Ivezić et al. 2002). According to NED,[16] SDSS J1136+0242 is not detected in any radio catalog besides FIRST; thus, no interesting constraint can be placed on its radio spectral index.

2.4. *Spectroscopy and Redshift Determination*

SDSS J1136+0242 was targeted for spectroscopy in the SDSS as a SERENDIPITY target (a category including FIRST sources fainter than $i = 19.1$; Stoughton et al. 2002) and as a high redshift quasar candidate.[17] The SDSS spectrum (Fig. 1) has a median signal-to-noise ratio (SNR) per pixel ranging from 4 in the *g* band to 7 in the *i* band. It shows a single, moderately broad Lyα emission line (FWHM$\simeq$1430 km s^{-1}) with accompanying Lyα and C IV absorption at three distinct redshifts within a velocity range of 2710 km s^{-1}. The curvature in the continuum between Lyα and $\sim$1280 Å is almost certainly due to two-photon emission from the 2^2S state of H I (see §2.5). The spectrum is well fit by the sum of two-photon emission and a power-law with $F_\lambda \propto \lambda^{0.15}$ (dashed lines; reduced chi-squared is $\chi^2_\nu = 1.106$, neglecting systematic errors in the spectrophotometry). This power-law spectral index is much redder than the $\alpha_\lambda = -0.4$ found by Steidel et al. (2002) for a sample of narrow-line, radio-quiet AGNs at $z \simeq 3$ or the $\alpha_\lambda = -1.56$ found for the typical SDSS quasar (Vanden Berk et al. 2001). In fact, less than 0.5% of SDSS quasars in the study of Richards et al. (2003) have such red continua.

To determine the systemic redshift of SDSS J1136+0242, we simultaneously fitted for the Lyα emission redshift, the Lyα absorption redshifts, and the C IV absorption redshifts using IRAF.[18] We assumed a single Gaussian profile for each component. Each line's width, height and center was allowed to vary independently. The Lyα absorption redshifts very closely matched the C IV absorption redshifts (Fig. 2), demonstrating that the Lyα emission does not bias the determination of the Lyα absorption systems' parameters. The best-fit Lyα emission redshift was identical to that of the highest redshift absorption system to within the errors. We therefore adopted the redshift of this system, $z = 2.4917 \pm 0.0009$, as the systemic redshift. (The other associated absorption systems are at $z = 2.4603 \pm 0.0004$ and $z = 2.4768 \pm 0.0002$.)

To place limits on emission line fluxes, we simultaneously fitted all broad emission and narrow absorption features listed in Table 2 to the rest-frame spectrum. The spectrum was first normalized by a single third-order spline fit to rest-frame spectral regions at 1090–2460 Å free of strong emission lines seen in normal quasars (inferred from Table 2 of Vanden Berk et al. 2001). Narrow absorption lines were allowed to vary in central wavelength, depth, and width, except as noted. Because of the obvious weakness of any emission lines besides Lyα, all broad emission lines were constrained to have the same width as Lyα. For N V and C IV doublet emission, we fit a single gaussian whose FWHM was the quadrature sum of the Lyα FWHM and the separation between the two doublet lines. Two fits to the emission lines were made: one where the central wavelength λ_{cen} was allowed to vary because AGN emission lines often exhibit velocity shifts (Richards et al. 2002b), and one where λ_{cen} was held fixed at the λ_{obs} values from Table 2 of Vanden Berk et al. (2001). We refer to those fits as the *variable*-λ_{cen} and *fixed*-λ_{cen} fits, respectively. Only the variable-λ_{cen} fit results are listed in Table 2, but line ratios for both fits are listed in Table 3 (see Appendix A).

As seen in Table 2, a few emission lines are nominally detected with rest-frame equivalent width (REW) values which are non-zero at $\gtrsim 3\sigma$ significance. These σ values do not include the uncertainties in the continuum fit, and so may be underestimates; however, we have also ignored the fact that the errors in the FWHM and the peak value are correlated, which will make the σ values overestimates. The differences between the fluxes from the variable-λ_{cen} and fixed-λ_{cen} fits are illustrative of the systematic uncertainties.

Because there is C IV absorption at the systemic redshift, the fit to the C IV emission line depends on the fit to the absorption. An unconstrained fit to the C IV spectral region yields considerable broad emission which is masked by relatively broad absorption (FWHM of 574 km s^{-1}). While we cannot completely rule out such a fit, we adopt a more plausible fit where the C IV absorption lines are constrained to have the same FHWM as the Lyα absorption at the same redshift (431 km s^{-1}). Even that width is probably an overestimate for the C IV absorption, as the other two associated systems have C IV widths only 20$-$40% as broad as Lyα. Nonetheless, this fit is conservative in the sense that narrower widths would further reduce the allowable C IV emission strength, moving this object even further from the norm for quasars.

[16] The NASA/IPAC Extragalactic Database (NED) is operated by the Jet Propulsion Laboratory, California Institute of Technology, under contract to NASA.

[17] Note that using the final version of the SDSS targeting software, SDSS J1136+0242 no longer qualifies as a high-redshift quasar candidate. SDSS J1136+0242 has colors red enough to place it very close to the stellar locus, and the SDSS quasar targeting algorithms are necessarily incomplete to such objects to avoid being swamped by false positives. Objects with lines as weak as SDSS J1136+0242 but with bluer (or much redder) continua will be targeted, but the SDSS is not complete to objects very similar to SDSS J1136+0242.

[18] The Image Reduction and Analysis Facility (IRAF) is distributed by the National Optical Astronomy Observatories, which is operated by AURA, Inc., under contract to the National Science Foundation.

2.5. *Hydrogen Two-Photon Emission and the Overall Spectrum*

The curvature in the continuum of SDSS J1136+0242 between Lyα and ∼1280 Å matches the characteristic spectral shape of forbidden two-photon emission from the 2^2S state of hydrogen (Aller 1984; Osterbrock 1989). The spectrum is well fit by the sum of two-photon emission and a power-law with $F_\lambda \propto \lambda^{0.15}$, and the SDSS photometry from the same epoch as the spectroscopy is also consistent with such a spectrum.[19] The $J-K_s$ color corresponds to a power-law spectrum of index $\alpha_\lambda = -0.14 \pm 0.30$, consistent within the uncertainties with an extrapolation of the value of $\alpha_\lambda = 0.15$ that fits the SDSS spectrum. The J and K_s magnitudes are fainter than an extrapolation of such a power-law; however, given the likelihood of flux variability between the optical and near-IR imaging epochs (Table 1), all the observations appear consistent with a spectrum which is the sum of two-photon emission and a rather red power-law.

It is important to remember that H I two-photon emission only occurs for electron densities $n_e \lesssim 10^4$ cm^{-3}. Above that density, collisions from the 2^2S state of hydrogen to the 2^2P state lead to Lyα emission ($2^2P \rightarrow 1^2S$) instead of two-photon emission ($2^2S \rightarrow 1^2S$). Thus, we are not seeing emission from gas with typical quasar broad-line region (BLR) densities ($\sim 10^{11}$ cm^{-3}).[20]

The ratio of the integrated two-photon continuum flux to the Lyα line flux (corrected for narrow Lyα absorption) in SDSS J1136+0242 is $F_{2q}/F_{Ly\alpha} = 4.60 \pm 0.66$. The intrinsic value of this ratio is $0.45 < F_{2q}/F_{Ly\alpha} < 0.58$ for $5{,}000\,\mathrm{K} < T < 20{,}000\,\mathrm{K}$ (Osterbrock 1989). Therefore, the Lyα emission flux in this object must have been reduced by a factor of at least 9 ± 1. The only plausible destruction mechanism is absorption by dust within the Lyα emission region, where resonant scattering of Lyα will increase its optical depth relative to the two-photon continuum. (Colisional deexcitation or bound-free ionization of the $n = 2$ level of hydrogen would affect Lyα and two-photon emission equally.)

Assuming the UV continuum is extincted by the Lyα-emitting gas, the maximum plausible extinction corresponds to a color excess of $E(B-V) = 0.15$, using the Small Magellanic Cloud extinction curve of Pei (1992). That extinction is the amount required to turn the $\alpha_\lambda = -1.56$ spectral slope of a typical SDSS quasar (Vanden Berk et al. 2001) into the estimated underlying UV spectral slope of $\alpha_\lambda = 0.15$ in SDSS J1136+0242. Extinction by $E(B-V) = 0.15$ would reduce $F_{2q}/F_{Ly\alpha}$ by a factor of 1.9 — the Lyα flux would be reduced by a factor of 2.7 and the two-photon continuum by a factor of 1.4 in total.[21] The additional required reduction of Lyα corresponds to an optical depth to scattering only 5.1 times greater in Lyα than in the adjacent continuum, which is easily achieved (Korista & Ferland 1998). However, while a reddened normal quasar spectrum plus reddened two-photon emission is an acceptable fit to the spectrum longward of Lyα ($\chi^2_\nu = 1.187$) and to the J-band flux, it underpredicts the K_s-band flux (rest-frame 6200 Å) by a factor of two. SDSS J1136+0242 is too luminous for this discrepancy to be explained by host galaxy emission, and the relative contributions of the Balmer continuum in the observed J band and the Paschen continuum in the observed K_s band will make the $J-K_s$ color bluer, not redder, for all reasonable power-law indices (Fig. 4.1 of Osterbrock 1989).

3. EXPLAINING SDSS J1136+0242

In this section we consider possible explanations for the unusual properties of SDSS J1136+0242. One discounted possibility is that this object is a gravitationally lensed Lyman-break galaxy (see Appendix B).

We first summarize our conclusions regarding the spectrum of SDSS J1136+0242 so far. A low-metallicity but dusty ($E(B-V) \lesssim 0.15$) narrow-line region with $n_e \lesssim 10^4$ cm^{-3} is responsible for the weak Lyα emission and strong two-photon continuum which contributes ≥30% of the continuum flux at 1500 Å. The underlying UV-optical continuum is well fit as a power-law with $F_\lambda \propto \lambda^{0.15}$, much steeper than usual for AGN, though an intrinsically bluer power-law plus reddening cannot be entirely ruled out. The emission-line flux of C IV is ≲5% of the Lyα flux, compared to typical values of ∼25% in quasars (Vanden Berk et al. 2001) and ∼15% in powerful radio galaxies (De Breuck et al. 2000). The Lyα linewidth is intermediate between these two classes of objects. The continuum is at best very weakly polarized. Stellar emission cannot contribute significantly to the continuum for the same reasons the lensed Lyman-break galaxy hypothesis was rejected (see Appendix B). We appear to be observing a featureless, power-law UV spectrum plus Lyα and H I two-photon emission from dusty gas.

3.1. *SDSS J1136+0242 as an Unusual Narrow-Line Radio Galaxy*

It may be reasonable to think of SDSS J1136+0242 as the spectrum of a radio galaxy plus a featureless continuum. The radio power of SDSS J1136+0242 is $P_{1.4\,\mathrm{GHz}} = 10^{34.15}$ erg s^{-1} Hz^{-1}, assuming $\alpha_\nu = -1.25$ near 1.4 GHz (De Breuck et al. 2000). This radio power is within an order of magnitude of those of the powerful $z > 2$ radio galaxies studied by De Breuck et al. (2000). SDSS J1136+0242 is radio-loud as defined by Ivezić et al. (2002), with a logarithmic radio-optical flux ratio $R_i = 1.43$ sufficient to place it at or above the traditional $R_i = 1$ division even in the presence of reddening with $E(B-V) = 0.15$.

The Lyα/C IV flux ratio of SDSS J1136+0242 would be extreme, but not unprecedented, for a narrow-line radio galaxy. The studies of De Breuck et al. (2000, 2001) include four objects out of ∼50 with larger Lyα/C IV flux ratios. Their Lyα emission is usually spatially extended, but the Lyα emission of SDSS J1136+0242 could also be extended since SDSS spectra are obtained through 3″ diameter fibers. The most likely explanation for the small C IV/Lyα ratio in those objects, and in SDSS J1136+0242 if this model is correct, is a low metallicity of $0.1\,Z_\odot$ or less in the line-emitting gas (Fig. 17 and §5.6 of De Breuck et al. 2000).

The Lyα emission FWHM of SDSS J1136+0242 would also be extreme, but not unprecedented, for a distant radio galaxy. SDSS J1136+0242 has a FWHM larger than all but two objects

[19] The photometry from the earlier photometric epoch, when the object was fainter, is better fit with a redder power-law index ($\alpha_\lambda = 0.30$).

[20] It is possible that the match of the spectral shape of SDSS J1136+0242 to that of the H I two-photon continuum is coincidental, since accretion disk spectra are not expected to be pure power-laws (Hubeny et al. 2000). If so, then we could be seeing emission from a BLR with $n_e > 10^4$ cm^{-3} but with unusual parameters that suppress emission from lines other than Lyα. We relegate further discussion of this rather unlikely possibility to Appendix A, and assume we have in fact detected two-photon emission throughout the rest of the main text.

[21] Emission at wavelength λ from a slab with total optical depth τ_λ at that wavelength will be reduced by a factor of $\tau_\lambda/(1-e^{-\tau_\lambda})$ from the $\tau = 0$ case.

in the sample of 52 studied by Baum & McCarthy (2000), both of which were among the 10 $z > 1$ objects in the sample. A study of $z \sim 2.5$ radio galaxies by van Ojik et al. (1997) found Lyα FWHMs of 670–1575 km s^{-1}, with the largest FWHM in small radio sources (<50 kpc). Additionally, Lyα absorption was seen in 9 of 10 small radio sources, but in only 2 of 8 radio sources larger than 50 kpc. Thus, the large Lyα emission FWHM and presence of Lyα absorption in SDSS J1136+0242 is consistent with it being a compact radio galaxy.

The Lyα luminosity of SDSS J1136+0242 is not exceptional. Lyα-emitting halos are often seen around powerful radio galaxies (van Ojik et al. 1997) and radio-loud quasars (Bremer et al. 1992), and occasionally around radio-quiet quasars (Bergeron et al. 1999; Bunker et al. 2003). The observed Lyα luminosity of SDSS J1136+0242 is 1.18×10^{43} erg s^{-1}, and even the inferred intrinsic Lyα luminosity (see §2.5) of 1.06×10^{44} erg s^{-1} is a factor of 10 below the largest Lyα luminosities seen in radio galaxies (Villar-Martín et al. 2003).

The luminosity of the two-photon continuum is nearly unprecedented, however. If only the two-photon continuum and Lyα were observed, SDSS J1136+0242 would still have $r = 21.5$, a magnitude equalled by fewer than a handful of powerful radio galaxies at $2 \leq z \leq 3$ (Chambers, Miley, & van Breugel 1988; Pentericci et al. 1997; De Breuck et al. 2001). The K_s magnitude of SDSS J1136+0242 ties with the brightest observed among powerful radio galaxies at $2 \leq z \leq 3$ in the sample of Willott et al. (2003) and is $\simeq 1\overset{\mathrm{m}}{.}25$ brighter than their best-fit $K-z$ relation. Two-photon continuum is not usually considered to be the dominant explanation for the UV continua of powerful radio galaxies. However, it clearly contributes a similar fraction of the continuum luminosity in some radio galaxies as it does in SDSS J1136+0242 (Vernet et al. 2001), and the fact that dust mixed with the emitting gas can modify the characteristic shape of the two-photon continuum may mean that it is more common than has been concluded from analyses that neglect that effect.

The volume V of the region emitting the Lyα line and the two-photon continuum can be estimated using the relation $L_{Ly\alpha} = 4 \times 10^{-24} n_e^2 f V$ erg s^{-1} (Villar-Martín et al. 2003) with the constraint that $n_e \leq 10^4$ cm^{-3}. Relevant estimates of the filling factor of the Lyα-emitting gas, f, range from 10^{-4} to 10^{-8} (§ 4.2.4 of Villar-Martín et al. 2003), but if we apply the above equation to the intrinsic $L_{Ly\alpha}$ inferred from the SDSS spectroscopy then f must be such that the emission region in SDSS J1136+0242 is smaller in angular size than the SDSS fiber diameter of 3″ (corresponding to 11.8 kpc at $z = 2.4917$). Assuming a typical radio galaxy narrow-line region (NLR) with $n_e = 10^2$ cm^{-3} (Villar-Martín et al. 2003), a relatively high filling factor of $f > 2.5 \times 10^{-5}$ is inferred. Spatially resolved observations of the Lyα emission would clearly be useful to clarify its origin and to jointly constrain the density and filling factor of the Lyα-emitting gas.

One important difference between SDSS J1136+0242 and the brightest $z \simeq 2.5$ radio galaxies is that at least some of the latter objects have much higher polarizations (5-10% vs. <1% for SDSS J1136+0242; Vernet et al. 2001). This difference can be explained if SDSS J1136+0242 is viewed close to face-on, unlike most powerful radio galaxies. Such a viewing angle maximizes the symmetry of any scattering, thereby decreasing the observed polarization. For a biconical scattering region geometry with opening half-angle 45° and a maximum $P = 17\%$ at a viewing angle from the cone axis of $\vartheta = 90°$, an observed $P < 1\%$ is possible at $\vartheta < 8°$ (Manzini & di Serego Alighieri 1996). The larger the opening angle of the bicones, the larger the range of ϑ for which $P < 1\%$, and of course $P = 0\%$ for a spherical scattering region.

3.2. *Possible Origins of the Featureless UV Continuum*

The scenario outlined above for SDSS J1136+0242 — a face-on radio galaxy with an extended, dusty, low-metallicity, Lyα-emitting NLR — explains many of its characteristics. We now discuss possible explanations for why we see a luminous, featureless, and variable ultraviolet continuum but no emission from the broad-line region, properties which are not immediately explained by this model.

- The observed variability, among other arguments, rules out a stellar origin for the observed UV continuum (see Appendix B).
- If by chance a gap in the obscuring matter enables us to see the continuum source in this object, we should also see emission from the broad-line region unless the gap is very small (since the continuum source is smaller than the BLR) or the BLR produces unusually weak lines (see Appendix A). Some broad absorption line (BAL) quasars have very weak metal emission lines, but no BAL outflow has ever been seen to absorb emission lines without also strongly absorbing the continuum.
- A related possibility is that we *are* seeing the continuum source and the BLR, but that the latter has a very high density of $n_H \gtrsim 10^{13}$ cm^{-3} and has thermalized so that it emits only blackbody radiation. The dominant range of temperatures expected for such emission is $6000 \lesssim T \lesssim 10000$ K (Ferland 1999), and our photometry covers the peak wavelengths of such blackbodies. There is no clear sign of such emission in the photometry or spectroscopy. It is true that blackbody emission could help explain the deficit of K_s-band flux found when the spectrum is modeled as a reddened power-law with $\alpha_\lambda = -1.56$ (§2.5), but the temperature of such putative emission would have to be 4000 K $\lesssim T \lesssim$ 5500 K. This is too narrow a temperature range, and too far below the expected temperatures, to be considered a detection of thermalized BLR emission.
- Perhaps we have an unobscured sightline to a central engine which simply lacks a BLR. For example, Nicastro, Martocchia, & Matt (2003) have suggested that AGN with accretion rates $< 10^{-3}$ of the Eddington rate might lack broad lines. But if SDSS J1136+0242 was accreting at such a low rate, explaining its observed luminosity would require an implausibly large black hole mass of $\gtrsim 10^{11.4}\ M_\odot$ (Peterson 1997; McLure & Dunlop 2004). Thus, a different explanation than that of Nicastro et al. (2003) would need to be found if SDSS J1136+0242 is shown to lack a BLR.
- Seyfert 2 galaxies are known to have an unpolarized, featureless UV continuum which is not attributable to starlight, but is plausibly due to optically thin free-free emission (Tran 1995). However, this emission component usually arises from outside the broad-line region, where any variability timescale should be longer than the rest-frame 40-70 days observed in SDSS J1136+0242. Moreover, this emission component typically accounts for only ∼4% of the total UV flux of a

Seyfert 1 galaxy, whereas it would have to account for ∼70% of the UV flux in SDSS J1136+0242.

- The continuum could be relativistically beamed synchrotron emission from a jet pointing nearly along our line of sight. The beaming factor must be at least ∼15 to explain the low equivalent widths of C IV and C III]. Beaming would be consistent with the face-on orientation of SDSS J1136+0242 invoked to explain the absence of highly polarized scattered light. While synchrotron-dominated objects (blazars) usually have high intrinsic polarizations, there are at least two possible explanations for why that is not the case here. One is that such polarization is highly variable: some BL Lac objects with $P > 3\%$ at one epoch have been seen to have $P < 1\%$ at another epoch (Jannuzi, Smith, & Elston 1993; Visvanathan & Wills 1998). The other is that the synchrotron emission in blazars typically arises from several emission regions, and that unless those regions have aligned polarization vectors the overall polarization will be reduced (§ 4.1.1 of Lister & Smith 2000). However, there are two strong arguments against this beaming hypothesis. First, the spectral energy distribution (SED) of SDSS J1136+0242 is much steeper between radio and UV frequencies than is the case for blazars (Fig. 12 of Fossati et al. 1998). Second, blazars are typically polarized parallel to the radio jet axis, because the synchrotron emission arises in shocks where compression yields magnetic fields oriented perpendicular to the jet flow (recall that the polarization and magnetic field vectors are perpendicular). But in SDSS J1136+0242, if we identify the radio major axis (§2.3) as the jet axis then the polarization is consistent with being perpendicular to it ($\Delta\theta = 81 \pm 20^\circ$).

- SDSS J1136+0242 may be a higher-redshift, lower-luminosity analog of the quasar PG 1407+265 (McDowell et al. 1995), which has very weak, very broad, highly blueshifted high-ionization emission lines (C IV has REW=4.6±2 Å and is blueshifted by $10200 \pm 1200\,\mathrm{km\,s^{-1}}$ from Hα; both lines have a FWHM of $\simeq 7000\,\mathrm{km\,s^{-1}}$). The SED of PG 1407+265 is a very good match to the median radio-quiet quasar SED of Elvis et al. (1994), and so its weak lines cannot be explained by a very soft ionizing continuum (Leighly, Halpern, & Jenkins 2004) or a relativistically beamed continuum. Nonetheless, Blundell, Beasley, & Bicknell (2003) have presented strong evidence for the existence of a relativistic jet in PG 1407+265 oriented very close to our line of sight. Unlike most blazars, PG 1407+265 has a very low polarization of $P = 0.24 \pm 0.16\%$ at a position angle roughly perpendicular to the jet axis ($\Delta\theta = 70 \pm 20^\circ$, assuming the jet axis is the A-B axis in Blundell et al. 2003). These observations place PG 1407+265 in the class of low-polarization radio quasars (Lister & Smith 2000). Such objects are thought to represent quiescent blazars whose jets do not harbor strong shocks, resulting in magnetic fields which are not necessarily oriented perpendicular to the flow.

PG 1407+265 and SDSS J1136+0242 are similar in that they have weak UV emission lines, low polarizations apparently oriented perpendicular to the radio jet axis, and nearly face-on orientations. It is not known why PG 1407+265 has such unusual emission-line properties,[22] but whatever the explanation is, it may apply to both objects. If SDSS J1136+0242 is similar to PG 1407+265, we expect that optical spectra with a higher SNR will reveal very broad, weak, highly blueshifted emission lines and that near-IR spectra will reveal strong Fe II emission (McDowell et al. 1995). In addition, as a low-polarization radio quasar, SDSS J1136+0242 should have a radio core with the same, low polarization as the optical continuum and with the same polarization position angle roughly perpendicular to the jet axis.

4. CONCLUSION

The newly discovered, radio-loud AGN SDSS J1136+0242 is unusual in possessing a strong continuum without accompanying strong metal-line emission. Of ∼2400 quasars in the SDSS Data Release 1 quasar catalog (Schneider et al. 2003) with $z \geq 2.12$, sufficient to place Lyα within the spectral coverage of the SDSS spectrographs, it is the only object with strong, relatively narrow Lyα emission and no accompanying metal-line emission (excepting broad absorption line quasars where such emission is absorbed along with part or all of the continuum).

The spectrum of SDSS J1136+0242 can generally be understood as that of a very optically luminous radio galaxy, in terms of Lyα emission flux, velocity width, associated narrow Lyα and C IV absorption, C IV/Lyα ratio (from a low-metallicity NLR), and even two-photon continuum strength (§2.5 and §3.1).

However, SDSS J1136+0242 has a very strong UV continuum not seen in radio galaxies (§3.2). This continuum is unpolarized, suggesting a face-on orientation for SDSS J1136+0242. The continuum could be relativistically beamed synchrotron emission which swamps the intrinsic broad-line emission, but the SED of SDSS J1136+0242 is not a good match to known synchrotron-dominated objects. A more likely possibility is that SDSS J1136+0242 is a PG 1407+265 analog: a low-polarization radio quasar which for some unknown reason has very weak, very broad, highly blueshifted high-ionization emission lines. A better optical spectrum is needed to determine if such features are present in SDSS J1136+0242. This scenario predicts polarization perpendicular to the axis of the radio jet, which is tentatively observed to be the case in both SDSS J1136+0242 and PG 1407+265 but requires confirmation with better polarization data.

In the unlikely event the Lyα is from a broad-line region of typical density, the dip in the continuum otherwise attributed to H I two-photon emission is unexplained. Also, the BLR would have to consist predominantly of low-ionization or low-metallicity gas (Appendix A). If the former, it is unclear what about SDSS J1136+0242 causes its lack of the high-ionization gas which dominates the broad-line regions of most AGNs. If the latter, metallicities $\lesssim$1% of solar are required.

Further investigation of SDSS J1136+0242 would benefit from better optical spectra (preferably spatially resolved to

[22] A small number of 'lineless' quasars have been identified (Fan et al. 1999; Anderson et al. 2001; Leighly et al. 2004) which have weak emission lines for reasons apparently unrelated to relativistic beaming, but which may be extreme examples of the Baldwin effect. However, SDSS J1136+0242 is not luminous enough for its weak line emission to be plausibly explained by the Baldwin effect, even accounting for the large scatter in that relation — SDSS J1136+0242 is 2.5 times less luminous than PG 1407+265 and yet has a C IV REW two times smaller.

search for and measure any spatial extent of Lyα), better optical polarimetry (or at least another epoch of the same quality), deep, high-resolution radio imaging and polarimetry to determine the jet axis, near-IR spectroscopy to study the rest-frame optical spectrum, and multiwavelength photometry to determine if its spectral energy distribution can be reconciled with those of blazars.

We thank D. Johnston, M. Brotherton, M. De Robertis, J. Krolik, G. Richards, C. Ryan, S. Savaglio, M. SubbaRao, P. Wiita and J. Willis for comments and assistance. PBH acknowledges support from Fundación Andes and the Department of Astrophysical Sciences at Princeton University, EH & KG from the David and Lucille Packard Foundation, DPS from NSF grant AST03-07582, and MNO from the REU program via a supplement to NSF grant AST-0071091 to Princeton University. Funding for the creation and distribution of the SDSS Archive has been provided by the Alfred P. Sloan Foundation, the Participating Institutions, the National Aeronautics and Space Administration, the National Science Foundation, the U.S. Department of Energy, the Japanese Monbukagakusho, and the Max Planck Society. The SDSS Web site is http://www.sdss.org/. The SDSS is managed by the Astrophysical Research Consortium (ARC) for the Participating Institutions: The University of Chicago, Fermilab, the Institute for Advanced Study, the Japan Participation Group, The Johns Hopkins University, Los Alamos National Laboratory, the Max-Planck-Institute for Astronomy (MPIA), the Max-Planck-Institute for Astrophysics (MPA), New Mexico State University, University of Pittsburgh, Princeton University, the United States Naval Observatory, and the University of Washington.

APPENDIX

AN UNUSUAL BROAD-LINE AGN?

If the match of the spectral shape of SDSS J1136+0242 to that of the H I two-photon continuum is coincidental, we might be seeing emission from a BLR with $n_e > 10^4$ cm^{-3} and unusual parameters that suppress emission from lines other than Lyα.

Ferland (1999), hereafter F99, discuss the line emission from a single quasar broad-line region gas cloud as a function of many different physical parameters. C IV emission is an important coolant in photoionized gas, and so weak C IV emission indicates gas with low metallicity ($\log Z/Z_\odot \leq -1$), low ionization ($\log U \leq -2$), or both. Tentative emission line flux ratios and limits for SDSS J1136+0242 are listed in Table 3, along with ratios from two photoionization simulations given in F99. Figure 3 compares several sets of line ratios: solid triangles (with 1σ error bars) are the variable-λ_{cen} measurements, open triangles are the fixed-λ_{cen} measurements, crosses are from a low metallicity simulation ($\log Z/Z_\odot = -2$), open squares are from a low ionization parameter simulation ($\log U = -3$, where U is the ratio of the photon density at the cloud's illuminated face to the hydrogen nucleus density n_H), and half-filled squares are estimates of a low ionization parameter simulation with a density $n_H = 10^{11}$ cm^{-3} instead of the baseline $n_H = 10^{10}$ cm^{-3} (see below).

The low-metallicity model is reasonably consistent with the data, but would be strongly rejected if the nominal detection of Al III in the variable-λ_{cen} fit is correct. (The fixed-λ_{cen} fit yields only an upper limit on Al III.) Note that the presence of associated C IV absorption with saturated line ratios does *not* rule out the low-metallicity model. Even low metallicity C IV absorption systems are often saturated at the SDSS spectral resolution, and the associated absorption systems often seen in AGN can be located in nearby galaxies or in host galaxy disks or halos, as well as near the nucleus (Hamann & Ferland 1999).

Of the models plotted, the line ratios of SDSS J1136+0242 are most consistent with emission from low-ionization, high-density clouds. The greatest discrepancy ($2-3\sigma$) in that scenario is that Si III] is predicted to be $\sim$10 times stronger than observed. Nonetheless, it is preferred over the normal density low-ionization simulation because the latter predicts too strong a C III] line, at the $4-6\sigma$ level.

If we adopt the locally optimally-emitting cloud model pioneered by Baldwin et al. (1995), in which the emitting gas is assumed to span a wide range in density and distance (and therefore ionization parameter), a low metallicity scenario is preferable. Otherwise, we would have to explain why gas exists close to the black hole (to produce the UV continuum source) and far away from it (to produce low-ionization emission), but not at intermediate distances where broad metal-line emission is normally produced.

A LENSED LYMAN-BREAK GALAXY?

We were initially enamored of the possibility that SDSS J1136+0242 could be a lensed Lyman-break galaxy (LBG) similar to MS1512-cB58 (Yee et al. 1996), but with Lyα in emission. This was due in part to its spectrum being radically different from a typical broad-line AGN and in part to the dip in the spectrum between Lyα and $\sim$1280 Å, which is not generally seen in quasars but is seen in LBGs (Shapley et al. 2002). However, the evidence against lensing is overwhelming.

First, SDSS J1136+0242 is photometrically variable at the 99.8% confidence level, with $\Delta m_{AB} = 0.08 \pm 0.02$ (averaged over five bands) over 67 rest-frame days. Such variability is common in AGN but would be inexplicable for a Lyman-break galaxy.

Second, SDSS J1136+0242 is unresolved in the SDSS *ugriz* imaging and in *J* imaging obtained on UT 2003 April 19 at the Canada-France-Hawaii Telescope (CFHT) with the CFHTIR camera. In the CFHT image, SDSS J1136+0242 has FWHM=0.″59, compared to FWHM=0.″60 $\pm$ 0.″01 measured from 6 stars in the same image. A double-image lens with separation 0.″2 would have a FWHM=0.″63 in 0.″60 seeing, and so lensing with separation $\geq$ 0.″2 is ruled out at the $\sim 3-4\sigma$ level. This does not necessarily rule out a high magnification lens — for example, APM 08279+5255 has a separation of 0.″378 and a magnification of $\sim 40-90$ (Ibata et al. 1999) — but it does considerably narrow the parameter space accessible to such a lens. Similarly, a cluster-lens such as MS1512-cB58 is rendered unlikely by the non-detection of any other object within 11″ in either the CTIO, CFHT or SDSS imaging, to limits $\sim$3 magnitudes fainter than SDSS J1136+0242 in *i*, $\sim$2 magnitudes in *J*, and $\sim$1 magnitude in K_s. A lensing cluster would have to have a redshift $z \gtrsim 1$ to avoid detection in those data.

Third, the spectral properties of SDSS J1136+0242 are very different from those of LBGs. Its rest-frame UV spectral index ($\alpha_\lambda = 0.15$) is much redder than is typical for LBGs ($-1.09 < \alpha_\lambda < -0.73$; Shapley et al. 2002). And if it was a LBG, SDSS J1136+0242 would go against the trend found by Shapley et al. (2002) for the UV continuum to become bluer with increasing Lyα emission strength. Additionally, perusal of model UV spectra for a wide range of young stellar population models (Leitherer et al. 1999) reveals none with continua as featureless as that of SDSS J1136+0242.

We therefore conclude that SDSS J1136+0242 is not a lensed Lyman-break galaxy.

REFERENCES

Aller, L. H., ed. 1984, Physics of Thermal Gaseous Nebulae
Anderson, S. F., Fan, X., Richards, G. T., Schneider, D. P., Strauss, M. A., Vanden Berk, D. E., Gunn, J. E., Knapp, G. R., et al., 2001, AJ, 122, 503
Baldwin, J., Ferland, G., Korista, K., & Verner, D. 1995, ApJ, 455, L119
Baum, S. A. & McCarthy, P. J. 2000, AJ, 119, 2634
Becker, R. H., White, R. L., & Helfand, D. J. 1995, ApJ, 450, 559
Bergeron, J., Petitjean, P., Cristiani, S., Arnouts, S., Bresolin, F., & Fasano, G. 1999, A&A, 343, L40
Blanton, M. R., Lin, H., Lupton, R. H., Maley, F. M., Young, N., Zehavi, I., & Loveday, J. 2003, AJ, 125, 2276
Blundell, K. M., Beasley, A. J., & Bicknell, G. V. 2003, ApJ, 591, L103
Bremer, M. N., Fabian, A. C., Sargent, W. L. W., Steidel, C. C., Boksenberg, A., & Johnstone, R. M. 1992, MNRAS, 258, 23P
Bunker, A., Smith, J., Spinrad, H., Stern, D., & Warren, S. 2003, Ap&SS, 284, 357
Chambers, K. C., Miley, G. K., & van Breugel, W. J. M. 1988, ApJ, 327, L47
De Breuck, C., Röttgering, H., Miley, G., van Breugel, W., & Best, P. 2000, A&A, 362, 519
De Breuck, C., van Breugel, W., Röttgering, H., Stern, D., Miley, G., de Vries, W., Stanford, S. A., Kurk, J., et al., 2001, AJ, 121, 1241
Elvis, M., Wilkes, B. J., McDowell, J. C., Green, R. F., Bechtold, J., Willner, S. P., Oey, M. S., Polomski, E., et al., 1994, ApJS, 95, 1
Fan, X., Strauss, M. A., Gunn, J. E., Lupton, R. H., Carilli, C. L., Rupen, M. P., Schmidt, G. D., Moustakas, L. A., et al., 1999, ApJ, 526, L57
Ferland, G. 1999, in Quasars and Cosmology, eds. G. Ferland & J. Baldwin, (San Francisco: ASP), 147
Fossati, G., Maraschi, L., Celotti, A., Comastri, A., & Ghisellini, G. 1998, MNRAS, 299, 433
Fukugita, M., Ichikawa, T., Gunn, J. E., Doi, M., Shimasaku, K., & Schneider, D. P. 1996, AJ, 111, 1748
Gunn, J. E., Carr, M., Rockosi, C., Sekiguchi, M., Berry, K., Elms, B., de Haas, E., Ivezić , Ž., et al., 1998, AJ, 116, 3040
Hamann, F. & Ferland, G. 1999, ARA&A, 37, 487
Hamann, F., Korista, K. T., Ferland, G. J., Warner, C., & Baldwin, J. 2002, ApJ, 564, 592
Hogg, D., Finkbeiner, D., Schlegel, D., & Gunn, J. 2001, AJ, 122, 2129
Hubeny, I., Agol, E., Blaes, O., & Krolik, J. H. 2000, ApJ, 533, 710
Ibata, R. A., Lewis, G. F., Irwin, M. J., Lehár, J., & Totten, E. J. 1999, AJ, 118, 1922
Ivezić, Ž., Menou, K., Knapp, G. R., Strauss, M. A., Lupton, R. H., Vanden Berk, D. E., Richards, G. T., Tremonti, C., et al., 2002, AJ, 124, 2364
Jannuzi, B. T., Smith, P. S., & Elston, R. 1993, ApJS, 85, 265
Korista, K. & Ferland, G. 1998, ApJ, 495, 672
Leighly, K. M., Halpern, J. P., & Jenkins, E. P. 2004, to appear in AGN Physics with the Sloan Digital Sky Survey, eds. G. T. Richards & P. B. Hall, in press (astro-ph/0402535)
Leitherer, C., Schaerer, D., Goldader, J. D., Delgado, R. M. G., Robert, C., Kune, D. F., de Mello, D. F., Devost, D., et al., 1999, ApJS, 123, 3
Lister, M. L. & Smith, P. S. 2000, ApJ, 541, 66
Lupton, R. H., Gunn, J. E., & Szalay, A. S. 1999, AJ, 118, 1406
Manzini, A. & di Serego Alighieri, S. 1996, A&A, 311, 79
McDowell, J. C., Canizares, C., Elvis, M., Lawrence, A., Markoff, S., Mathur, S., & Wilkes, B. J. 1995, ApJ, 450, 585
McLure, R. J. & Dunlop, R. J. 2004, MNRAS, in press (astro-ph/0310267)
Morton, D. C., York, D. G., & Jenkins, E. B. 1988, ApJS, 68, 449
Nicastro, F., Martocchia, A., & Matt, G. 2003, ApJ, 589, L13
Osterbrock, D. E. 1989, Astrophysics of Gaseous Nebulae and Active Galactic Nuclei (Mill Valley: University Science Books)
Pei, Y. C. 1992, ApJ, 395, 130
Pentericci, L., Roettgering, H. J. A., Miley, G. K., Carilli, C. L., & McCarthy, P. 1997, A&A, 326, 580
Peterson, B. M. 1997, Active Galactic Nuclei (Cambridge: Cambridge University Press)
Pier, J. R., Munn, J. A., Hindsley, R. B., Hennessy, G. S., Kent, S. M., Lupton, R. H., & Ivezić, Ž. 2003, AJ, 125, 1559
Probst, R. G., Montane, A., Warner, M., Boccas, M., Bonati, M., Galvez, R., Tighe, R., Ashe, M. C., et al., 2003, in Instrument Design and Performance for Optical/Infrared Ground-based Telescopes, eds. M. Iye & A. F. M. Moorwood, Proceedings of the SPIE, 4841, 411–419
Richards, G. T., Fan, X., Newberg, H. J., Strauss, M. A., Vanden Berk, D. E., Schneider, D. P., Yanny, B., Boucher, A., et al., 2002a, AJ, 123, 2945
Richards, G. T., Vanden Berk, D. E., Reichard, T. A., Hall, P. B., Schneider, D. P., SubbaRao, M., Thakar, A. R., & York, D. G. 2002b, AJ, 124, 1
Richards, G. T., Hall, P. B., Vanden Berk, D. E., Strauss, M. A., Schneider, D. P., Weinstein, M. A., Reichard, T. A., York, D. G., Knapp, G. R., Fan, X., Ivezić, Ž., Brinkmann, J., Budavári, T., Csabai, I., & Nichol, R. C. 2003, AJ, 126, 1131
Schlegel, D. J., Finkbeiner, D. P., & Davis, M. 1998, ApJ, 500, 525
Schneider, D. P., Fan, X., Hall, P. B., Jester, S., Richards, G. T., Stoughton, C., Strauss, M. A., SubbaRao, M., et al., 2003, AJ, 126, 2579
Shapley, A. E., Steidel, C. C., Adelberger, K. L., & Pettini, M. 2002, in to appear in The New Era of Cosmology, eds. T. Shanks & N. Metcalfe (San Francisco: ASP)
Smith, J. A., Tucker, D. L., Kent, S., Richmond, M. W., Fukugita, M., Ichikawa, T., Ichikawa, S., Jorgensen, A. M., et al., 2002, AJ, 123, 2121
Steidel, C. C., Hunt, M. P., Shapley, A. E., Adelberger, K. L., Pettini, M., Dickinson, M., & Giavalisco, M. 2002, ApJ, 576, 653
Stoughton, C., Lupton, R. H., Bernardi, M. B., Blanton, M. R., Burles, S., Castander, F. J., Connolly, A. J., Eisenstein, D. J., et al., 2002, AJ, 123, 485
Strauss, M. A., Weinberg, D. H., Lupton, R. H., Narayanan, V. K., Annis, J., Bernardi, M., Blanton, M., Burles, S., et al., 2002, AJ, 124, 1810
Tran, H. D. 1995, ApJ, 440, 597
van Ojik, R., Roettgering, H. J. A., Miley, G. K., & Hunstead, R. W. 1997, A&A, 317, 358
Vanden Berk, D. E., Richards, G. T., Bauer, A., Strauss, M. A., Schneider, D. P., Heckman, T. M., York, D. G., Hall, P. B., et al., 2001, AJ, 122, 549
Vanden Berk et al., D. E. 2004, ApJ, 601, 692
Vernet, J., Fosbury, R. A. E., Villar-Martín, M., Cohen, M. H., Cimatti, A., di Serego Alighieri, S., & Goodrich, R. W. 2001, A&A, 366, 7
Villar-Martín, M., Vernet, J., di Serego Alighieri, S., Fosbury, R., Humphrey, A., & Pentericci, L. 2003, MNRAS, 346, 273
Visvanathan, N. & Wills, B. J. 1998, AJ, 116, 2119
Willott, C. J., Rawlings, S., Jarvis, M. J., & Blundell, K. M. 2003, MNRAS, 339, 173
Yee, H. K. C., Ellingson, E., Bechtold, J., Carlberg, R. G., & Cuillandre, J.-C. 1996, AJ, 111, 1783
York, D. G., Adelman, J., Anderson, J. E., Anderson, S. F., Annis, J., Bahcall, N. A., Bakken, J. A., Barkhouser, R., et al., 2000, AJ, 120, 1579

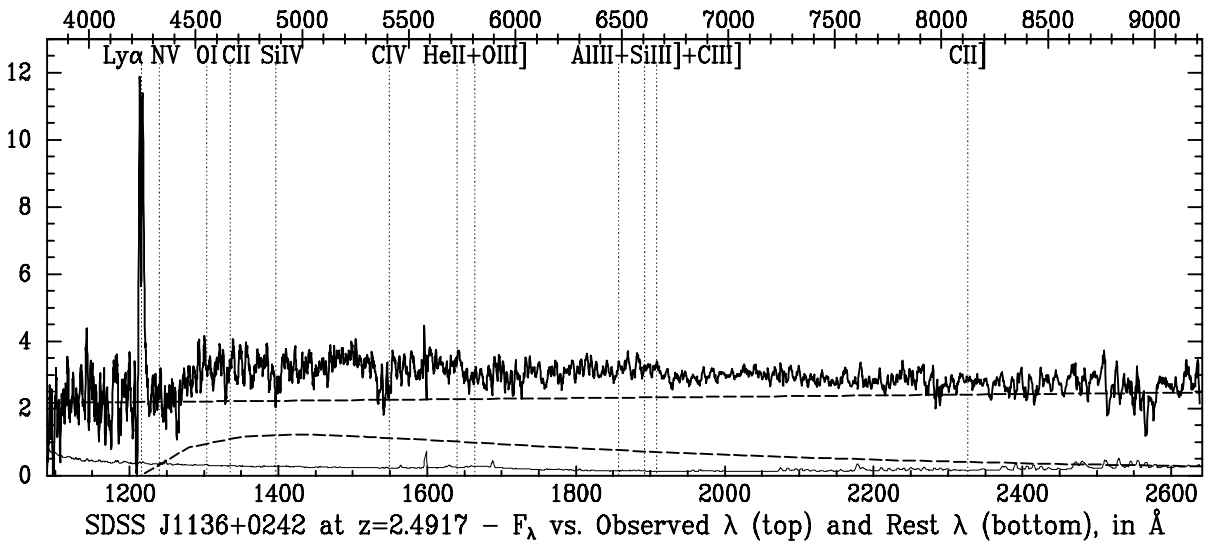

FIG. 1.— Full SDSS spectrum (resolution $R \simeq 2000$) of SDSS J1136+0242, smoothed by a 7-pixel boxcar filter, and accompanying 1σ uncertainties. The ordinate is F_λ in units of 10^{-17} ergs cm^{-2} s^{-1} Å^{-1}. Wavelengths of emission lines which are often strong in AGNs are marked, but only Lyα is unambiguously detected. The dashed lines show the decomposition of the continuum into a power law with $F_\lambda \propto \lambda^{0.15}$ plus H I two-photon continuum.

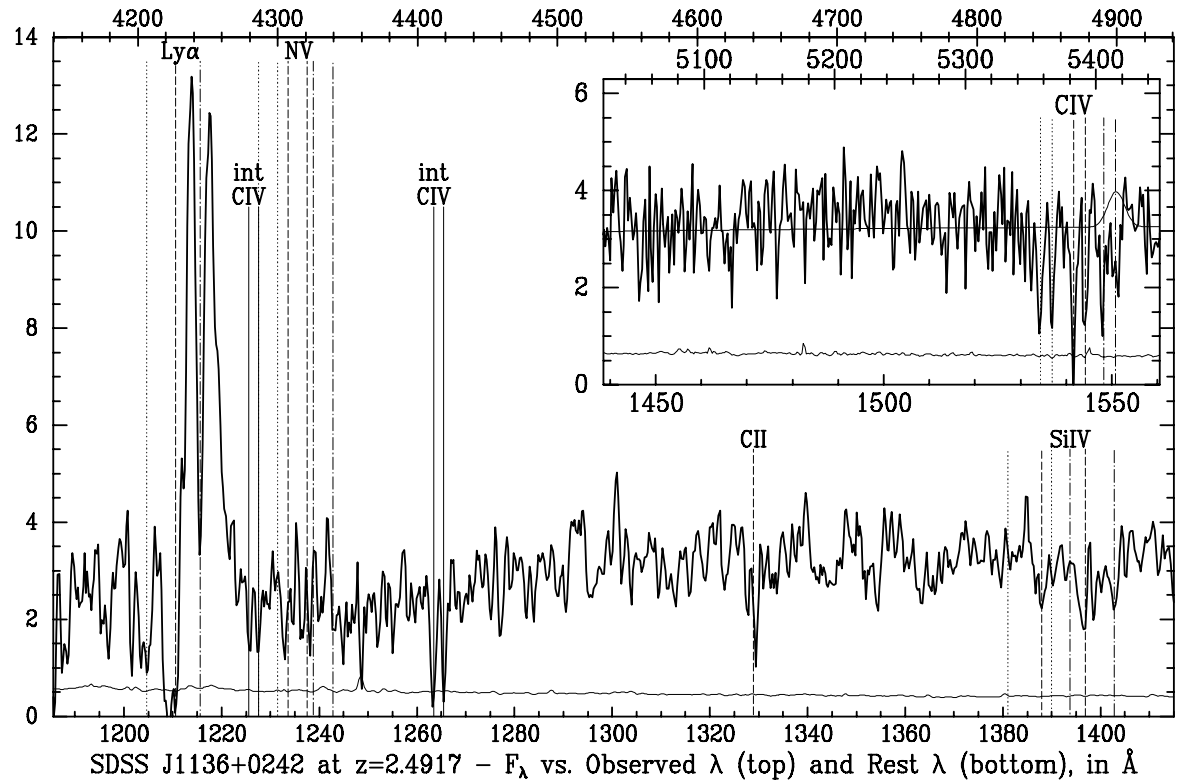

FIG. 2.— SDSS spectrum and 1σ uncertainties in regions of strong associated absorption. The ordinates are F_λ in units of 10^{-17} ergs cm^{-2} s^{-1} Å^{-1}. The three associated systems have C IV redshifts of $z = 2.4604$ (dotted), $z = 2.4768$ (dashed), and $z = 2.4917$ (dot-dashed). The vertical solid lines show intervening C IV systems. The inset shows the unsmoothed spectrum around C IV, along with the best-fit continuum and variable-λ_{cen} C IV emission line. The main panel shows the spectrum from Lyα to Si IV, smoothed by a 3-pixel boxcar. Si IV absorption (see Table 1) is most reliably detected at $z = 2.4768$ (dashed), and C II as well, although the latter is at a slightly higher redshift of $z = 2.4784$. N V is not detected at any of the three associated absorption redshifts, nor does it appear in emission.

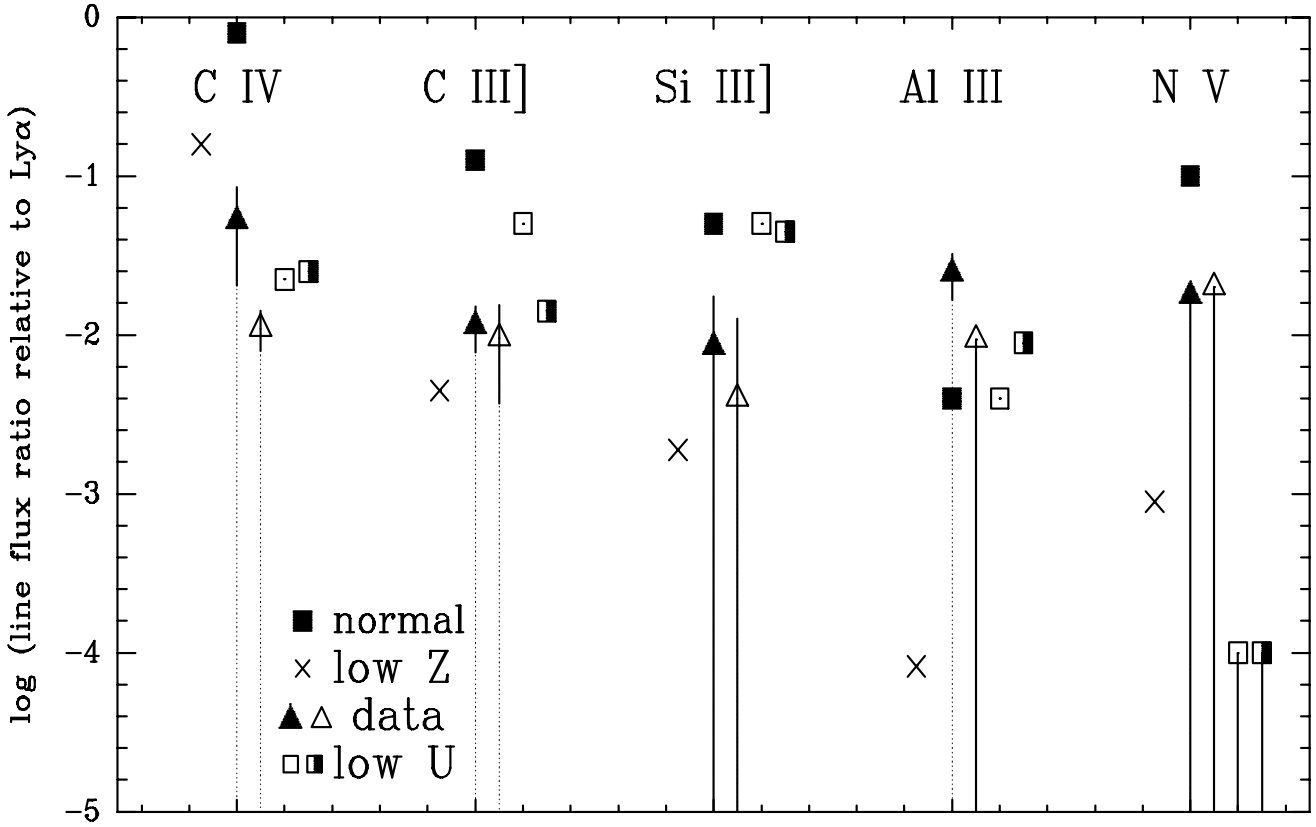

FIG. 3.— Line ratios for SDSS J1136+0242 and various photoionization simulations. Solid triangles (with 1σ error bars) are the variable-λ_{cen} measurements from Table 3, open triangles and error bars are fixed-λ_{cen} measurements, filled squares are from the baseline photoionization model of F99, crosses are from the low metallicity simulation ($\log Z/Z_{\odot} = -2$), open squares are from the low ionization parameter simulation ($\log U = -3$), and half-filled squares are estimates of a low ionization parameter simulation with a density $\log n_H = 11$ instead of the baseline $\log n_H = 10$. Solid lines extending off the bottom of the plot are limits consistent with zero. The dotted lines are reminders that the neither of the fits to the data allow the continuum to vary simultaneously with the lines, and thus all measurements may be upper limits.

TABLE 1
OBSERVATIONS OF SDSS J113658.36+024220.1

MJD of Observation	$u \pm \sigma_u$	$g \pm \sigma_g$	$r \pm \sigma_r$	$i \pm \sigma_i$	$z \pm \sigma_z$	$J \pm \sigma_J$	$K_s \pm \sigma_{K_s}$	20-cm, mJy	M_i	Spectroscopic plate/MJD-fiber
51009	···	···	···	···	···	···	···	1.44±0.15	···	···
51668	22.44±0.37	20.69±0.04	20.06±0.03	19.61±0.03	19.28±0.08	···	···	···	−26.30	···
51901	21.92±0.17	20.54±0.03	19.97±0.02	19.60±0.03	19.12±0.07	···	···	···	−26.31	···
51989	···	20.50±0.17	19.86±0.13	19.45±0.11	···	···	···	···	−26.46	513/51989-503
52670	···	···	···	···	···	18.93±0.11	17.77±0.14	···	···	···

Note. — Optical magnitudes are SDSS PSF magnitudes (Stoughton et al. 2002) except for MJD 51989, when they are equivalent magnitudes synthesized from the spectrophotometry as described in Vanden Berk et al. (2004). To match the optical, the near-IR magnitudes were measured in 7.″4 apertures. All magnitudes are on the AB system but have not been corrected for Galactic extinction; the Galactic $E(B-V)$ is 0.02 (Schlegel, Finkbeiner, & Davis 1998). The 20 cm column gives the integrated 20 cm flux density in milli-Janskies (mJy) from the FIRST survey (Becker et al. 1995). The absolute magnitude M_i was computed assuming $\alpha_{\lambda} = -1.5$ (Schneider et al. 2003).

TABLE 2

SDSS J1136+0242 LINE DETECTIONS AND LIMITS

Line	λ_{rest} [a]	Redshift	FWHM[b]	REW[c]	Flux[d]
		Emission Lines			
Lyα	1215.6701	2.4908±0.0006	1430±60	−33.8±3.4	315±32
N V	1240.14	2.584±0.002	(1720)	< -0.57	<5.5
O I	1304.35	2.483±0.003	(1430)	−1.71±0.41	17.4±4.2
C II	1335.30	2.500±0.003	(1430)	−1.41±0.34	14.7±3.6
Si IV	1393.755	2.507±0.004	(1430)	< -1.27	<13.8
Si IV	1402.770	2.507±0.026	(1430)	−0.88±0.82	9.6±8.9
C IV	1549.06	2.496±0.003	(1510)	−1.47±0.89	16.7±10.1
He II	1640.42	2.495±0.006	(1430)	−0.66±0.31	7.5±3.5
O III]	1663.48	2.478±0.004	(1430)	< -0.32	<3.6
Al III	1854.716	2.499±0.007	(1430)	−0.19±0.29	2.1±3.5
Al III	1862.79	2.504±0.002	(1430)	−0.70±0.22	7.7±2.4
Si III]	1892.03	2.500±0.003	(1430)	−0.25±0.26	2.7±2.8
C III]	1908.73	2.490±0.003	(1430)	−0.33±0.10	3.6±1.1
C II]	2326.44	2.493±0.012	(1430)	−0.42±0.36	4.0±3.4
		Associated Absorption Line Systems			
Lyα	1215.6701	2.4589±0.0011	510±160	1.43±0.56	···
C IV	1548.202	2.4602±0.0003	226±50	0.84±0.31	···
C IV	1550.774	2.4604±0.0001	155±77	0.61±1.29	···
Lyα	1215.6701	2.4771±0.0012	910±150	7.07±1.53	···
C II	1334.5323	2.4784±0.0006	180±130	0.63±0.49	···
Si IV[e]	1393.755	2.4769±0.0001	112±30	0.27±0.35	···
Si IV[e]	1402.770	2.4760±0.0048	250±260	0.55±0.90	···
C IV	1548.202	2.4768±0.0002	188±35	1.03±0.22	···
C IV	1550.774	2.4769±0.0003	212±71	0.91±0.36	···
Lyα	1215.6701	2.4914±0.0001	431±37	10.1±1.1	···
Si IV[e]	1393.755	2.4951±0.0002	62±21	0.18±0.12	···
Si IV[e]	1402.770	2.4918±0.0006	124±60	0.26±0.33	···
C IV	1548.202	2.4914±0.0004	(431)	1.12±0.44	···
C IV	1550.774	2.4921±0.0004	(431)	1.19±0.36	···
		Intervening Absorption Line Systems			
C IV	1548.202	1.7644±0.0006	77±56	0.58±1.10	···
C IV	1550.774	1.7637±0.0003	97±37	0.64±0.37	···
C IV	1548.202	1.8493±0.0003	(140±60)	1.34±0.58	···
C IV	1550.774	1.8494±0.0002	(140±60)	1.19±0.53	···
Mg II	2796.352	1.8497±0.0003	121±45	0.83±0.47	···
Mg II	2803.531	1.8499±0.0002	96±33	1.37±1.29	···

[a]Vacuum rest wavelength in Å (Morton, York, & Jenkins 1988). For emission lines, we used the λ_{lab} wavelengths given in Table 2 of Vanden Berk et al. (2001), except for cases of well-separated doublets.

[b]Rest-frame FWHM in km s^{-1}. For emission and associated absorption lines, the rest frame used is that of the quasar ($z = 2.4917$). For intervening absorption line systems, the rest frame is the weighted average C IV redshift of that system. Parentheses indicate fixed values that were not allowed to vary during at least the final iteration of the spectral fitting.

[c]Rest-frame equivalent width, in Å, of the Gaussian fit to the line. The rest frames are the same as those used for the FWHM calculation. Upper limits are 1σ.

[d]Flux of the Gaussian fit to each emission line, in units of 10^{-17} ergs cm^{-2} s^{-1}. Upper limits are 1σ.

[e]Only Si IV λ1402.770 is believably detected at $z = 2.4917$, which is unphysical since it is the weaker of the two lines of the doublet. Similarly, Si IV λ1402.770 appears stronger than Si IV λ1393.755 at $z = 2.4768$, which is again unphysical. Nevertheless, we include these absorption lines in our fit to the spectrum because doing so yields a more conservative upper limit on the Si IV emission. No other plausible identifications for these lines have been found (in particular, we can rule out Ni II at both known intervening C IV redshifts).

TABLE 3

SDSS J1136+0242 OBSERVED AND MODEL LOGARITHMIC LINE FLUX RATIOS

	C IV/Lyα	C III]/Lyα	Si III]/Lyα	Al III/Lyα	N V/Lyα	N V/He II	N V/C IV	C IV/He II	C IV/C III]	C III]/He II	C II]/C III]
Data, Variable-λ_{cen}	$-1.28^{+0.21}_{-0.41}$	$-1.94^{+0.12}_{-0.17}$	$-2.07^{+0.31}_{-\infty}$	$-1.61^{+0.12}_{-0.17}$	< -1.75	< -0.13	< -0.47	$0.35^{+0.25}_{-0.63}$	$0.68^{+0.24}_{-0.55}$	$-0.32^{+0.19}_{-0.35}$	$0.05^{+0.28}_{-1.01}$
Data, Fixed-λ_{cen}	$-1.96^{+0.11}_{-0.14}$	$-2.02^{+0.21}_{-0.41}$	$-2.4^{+0.5}_{-\infty}$	< -2.03	< -1.7	< 0.21	< -0.74	$-0.05^{+0.29}_{-1.38}$	$0.06^{+0.23}_{-0.51}$	$-0.11^{+0.21}_{-\infty}$	$0.14^{+0.27}_{-0.90}$
Low Metallicity	−0.8	−2.35	−2.725	−4.085	$\simeq -3.05$	···	···	···	···	···	···
Low Ionization	−1.65	−1.3	−1.3	−2.4	< -4	···	···	···	···	···	···

Note. — All "Data" values are the logarithms of the ratios of the line fluxes or limits. Low metallicity ($\log Z/Z_\odot = -2$) line ratios are from Figure 4 of F99 except for N V/Lyα, which also requires extrapolation from Figure 5 of Hamann et al. (2002). Low ionization ($\log U = -3$) line ratios are from Figure 6 of F99. Both sets of line ratios assume a power-law continuum with $\alpha_\nu = -1.5$ and density $n_H = 10^{10}$ cm^{-3}; the low-metallicity line ratios also assume $\log U = -1.5$.